Elsevier Editorial System(tm) for Clinical Neurophysiology
Manuscript Draft

Manuscript Number: CLINPH-D-08-2925R2

Title: Detection of experimental ERP effects in combined EEG-fMRI: evaluating the benefits of interleaved acquisition and Independent Component Analysis

Article Type: Full Length Article

Keywords: EEG-fMRI; ERP; ICA; gradient artifact; go-nogo, N2, P3.

Corresponding Author: Dr. Aureliu Lavric,

Corresponding Author's Institution: University of Exeter

First Author: Aureliu Lavric

Order of Authors: Aureliu Lavric; Nino Bregadze, PhD; Abdelmalek Benattayallah, PhD

Revision Note

ABSTRACT

Objective: The present study examined the benefit of rapid alternation of EEG and fMRI (a common strategy for avoiding artifact caused by rapid switching of MRI gradients) for detecting experimental modulations of ERPs in combined EEG-fMRI. The study also assessed the advantages of aiding the extraction of specific ERP components by means of signal decomposition using Independent Component Analysis (ICA).

Methods: 'Go-nogo' task stimuli were presented either during fMRI scanning or in the gaps between fMRI scans, resulting in 'gradient' and 'no gradient' ERPs. 'Go-nogo' differences in the N2 and P3 components were subjected to conventional ERP analysis, as well as single-trial and reliability analyses.

Results: Comparable N2 and P3 enhancement on 'nogo' trials was found in the 'gradient' and 'no-gradient' ERPs. ICA-based signal decomposition resulted in better validity (as indicated by topography), greater stability and lower measurement error of the predicted ERP effects.

Conclusions: While there was little or no benefit of acquiring ERPs in the gaps between fMRI scans, ICA decomposition did improve the detection of experimental ERP modulations.

Significance: Simultaneous and continuous EEG-fMRI acquisition is preferable to interleaved protocols. ICA-based decomposition is useful not only for artifact cancellation, but also for the extraction of specific ERP components.

Detection of experimental ERP effects in combined EEG-fMRI: evaluating the benefits of interleaved acquisition and Independent Component Analysis

Aureliu Lavric[1,2]*, Nino Bregadze[1] and Abdelmalek Benattayallah[2]

[1]Cognitive Neurophysiology Laboratory, School of Psychology, University of Exeter, UK

[2]Peninsula MR Research Centre, School of Psychology, University of Exeter, UK

Keywords: EEG-fMRI; ERP; ICA; gradient artifact; go-nogo.

***Corresponding author:**

Aureliu Lavric

School of Psychology

University of Exeter

Washington Singer Laboratories

Perry Road

Exeter EX4 4QG

United Kingdom

Tel: +44 (0)1392 264642

Fax: +44 (0)1392 264623

e-mail: A.Lavric@exeter.ac.uk

ABSTRACT

Objective: The present study examined the benefit of rapid alternation of EEG and fMRI (a common strategy for avoiding artifact caused by rapid switching of MRI gradients) for detecting experimental modulations of ERPs in combined EEG-fMRI. The study also assessed the advantages of aiding the extraction of specific ERP components by means of signal decomposition using Independent Component Analysis (ICA).

Methods: 'Go-nogo' task stimuli were presented either during fMRI scanning or in the gaps between fMRI scans, resulting in 'gradient' and 'no gradient' ERPs. 'Go-nogo' differences in the N2 and P3 components were subjected to conventional ERP analysis, as well as single-trial and reliability analyses.

Results: Comparable N2 and P3 enhancement on 'nogo' trials was found in the 'gradient' and 'no-gradient' ERPs. ICA-based signal decomposition resulted in better validity (as indicated by topography), greater stability and lower measurement error of the predicted ERP effects.

Conclusions: While there was little or no benefit of acquiring ERPs in the gaps between fMRI scans, ICA decomposition did improve the detection of experimental ERP modulations.

Significance: Simultaneous and continuous EEG-fMRI acquisition is preferable to interleaved protocols. ICA-based decomposition is useful not only for artifact cancellation, but also for the extraction of specific ERP components.

INTRODUCTION

Blood oxygen level dependent (BOLD) fMRI and EEG are the most widely employed non-invasive measurements of brain activity. BOLD fMRI, which is sensitive to local blood oxygenation, has the highest spatial resolution among all non-invasive functional imaging techniques. However, the discrepancy between the time-scale of neuronal processes (of the order of milliseconds) and the time-scale of haemodynamic processes (of the order of seconds) is a fundamental constraint on the ability of fMRI to resolve functionally relevant neural activity in time. In contrast, EEG is capable of high temporal resolution measurement of electrophysiological processes, but the spatial localisation of that activity is severely limited by the 'inverse problem'- determining a (high-dimensional) intra-cerebral distribution of local field potentials from a (low-dimensional) distribution of surface voltage measurements.

To attempt to 'get the best of both worlds', researchers have combined measurements of EEG and fMRI in cognitive paradigms (Bénar et al., 2007; Debener et al., 2005; Eichele et al., 2005; Liebenthal et al., 2003; Mantini et al., 2009; Mulert et al., 2004; Strobel et al., 2008; Warbrick et al., 2009). Although such concurrent acquisition of non-invasive brain activity measurements of high temporal resolution (ERPs) and high spatial resolution (fMRI) is promising, it is also challenging, because of the effect of integration on data quality. The effects of the EEG apparatus and electrode gel on MR/fMR image quality seem confined to the immediate vicinity of EEG electrodes, leads and gel (Iannetti et al., 2005; Mullinger et al., 2008), particularly at the most commonly used MR field strengths of 1.5 and 3 T (Mullinger et al., 2008). In contrast, the quality of

the EEG signal is severely compromised by concurrent fMRI. Two MR-related artifacts are especially detrimental: (1) pulse (or cardioballistic) artifact- voltages thought to be induced in EEG electrodes by scalp pulsation and head movement following each heartbeat in a large magnetic field (Debener et al., 2008), and (2) gradient artifact- voltages elicited by rapid switching of radio frequency excitation fields and spatial encoding gradient fields in fMRI (Anami et al., 2003). Pulse artifact is of physiological origin, which means that the experimenter has no control over its time-course. Moreover, since it contaminates the entire epoch between heartbeats, correction is the only viable option for its cancellation. In contrast, the parameters of gradient artifact, particularly its timing, are largely under the experimenter's control. This gives one the opportunity of alternating the acquisition of EEG and fMRI data, thus ensuring the presence of EEG stretches that are free of gradient artifact. If the alternating periods of EEG or fMRI data acquisition are sufficiently long (e.g. 10-30 s), one can isolate the EEG segments containing no gradient artifact and apply pulse artifact correction algorithms without having to correct for gradient artifact at all (e.g. Bonmassar et al., 2001; Liebenthal et al., 2003).

However, this 'slow' interleaved procedure has significant drawbacks. In particular, if the alternating periods of EEG or fMRI data acquisition are of the order of 30 s or so (Bonmassar et al., 2001) the resulting EEG and fMRI data are not associated with the same stimuli, making it impossible to correlate over time the ERP components such as Mismatch Negativity, Error-Related Negativity, P2, N2, P3, etc., with the corresponding fMRI signal (e.g. Bénar et al., 2007; Debener et al., 2005; Eichele et al., 2005; Liebenthal et al., 2003; Mantini et al., 2009; Warbrick et al., 2009). Reducing the

duration of the alternating periods of EEG or fMRI data acquisition to ~10 s allows one to investigate the ERP and fMRI responses to the same stimuli, by relating the amplitude of ERP components in groups of several trials to the corresponding cumulative BOLD fMRI signal changes (Liebenthal et al., 2003). However, because this procedure does not allow correlating the EEG and fMRI data over single trials, it restricts the kind of ERP paradigm it can be applied to. Indeed, correlating the two measurements over single trials (e.g. Debener et al., 2005; Eichele et al., 2005; Bénar et al., 2007; Mantini et al., 2009; Warbrick et al., 2009) has been one of the primary motivations for combining EEG and fMRI acquisition (see Debener et al., 2006, and Laufs et al., 2008, for reviews).

A more subtle approach to interleaving the EEG and fMRI data acquisition is to exploit the difference in the time-scales of the physiological processes being measured. While local field potentials (widely believed to be the substrate of EEG) require a sampling period of millisecond (or at least centi-second) order, the sluggish BOLD fMRI response (16 s) can be sampled as sparsely as once every 3-6 s. Since the whole-brain acquisition time for fMRI with the standard Echo-Planar Imaging (EPI) sequence is about 2-3 s, it is relatively straightforward to use sparse fMRI acquisition leaving brief (e.g. 0.5-2 s) scanning-free intervals uncontaminated by gradient artifact. This ‘fast’ interleaved procedure suits well the ERP technique, which is typically based on EEG segments of 1 s or less, and ensures that the statistical analyses in both modalities reflect the physiological responses to the same stimuli. Indeed, many combined EEG-fMRI studies have used it (Debener et al., 2005; Eichele et al., 2005; Mulert et al., 2004; Strobel et al., 2008).

However, the ‘fast’ interleaved procedure also has its limitations. The number of ERP trials and fMRI images is substantially reduced as a consequence of interleaving, thus affecting the SNR in both measurements. Furthermore, stimulus timing is non-trivial: one needs to present the stimuli in the gradient-free gaps while avoiding constant intervals between the stimuli and the fMRI scanning onsets (see Methods for details). Finally, the sampling of the BOLD response is not uniform. Thus, the question arises whether the benefits of the ‘fast’ interleaved procedure outweigh the costs, particularly as we (Bregadze and Lavric, 2006) and others (Becker et al., 2005; Bénar et al., 2007; Comi et al., 2005; Mantini et al., 2009; Warbrick and Bagshaw, 2008) have shown that ERP components can be reliably obtained from EEG containing gradient artifact. Furthermore, efforts to synchronise the phase of the EEG acquisition and MRI gradient switches (Anami et al., 2003; Mandelkow et al., 2006) and optimise the fMRI imaging sequence to create brief ‘plateaus’ of minimal temporal slope in the MR gradient fields for the EEG sampling (Anami et al., 2003; Freyer et al., 2009) have resulted in superior gradient artifact correction.

It seems therefore important to compare ERP components elicited by stimuli presented during fMRI scanning to those elicited by stimuli presented in the no-gradient (no-fMRI scanning) gaps. Becker et al. (2005) and Warbrick and Bagshaw (2008) have reported such comparisons. Both studies examined the amplitude of visual evoked potentials and found similar amplitudes and latencies of the P1 and N1 visual ERP components obtained from stretches of EEG contaminated by MRI gradient switching and from uncontaminated stretches. Among several tests of fMRI sequence parameters and EEG artifact correction, Warbrick and Bagshaw (2008) also compared two

procedures for gradient artifact correction- one based on artifact averaging (Allen et al., 2000) and the other based on Principal Components Analysis (Niazy et al., 2005). Both procedures were found to yield good correspondence between the amplitude and latency of the P1-N1 complex obtained from stretches with vs. without gradient artifact.

Nevertheless, some aspects of the influence of gradients on the measurement of ERPs require further scrutiny. While the feasibility studies focused on early visual ERP components, most ERP-fMRI studies to date examined longer-latency components (e. g. N2, P2 and P3, Error-Related Negativity, Bénar et al., 2007; Debener et al., 2005; Eichele et al., 2005; Mantini et al., 2009; Mulert et al., 2004; Strobel et al., 2008; Warbrick et al., 2009). More importantly, the feasibility work above has been concerned with the detection of ERP components (peaks), whereas cognitive neuroscientists tend to investigate modulations of the amplitude, latency and scalp distribution of these components by specific experimental manipulations. Because such experimentally-induced differences are smaller in magnitude and more variable than the peaks themselves, it is important to examine the effects of gradients on their detection, too.

The present study employed a well-characterised ERP paradigm (the 'go-nogo' paradigm, Eimer, 1993; Falkenstein et al., 1999; Lavric et al., 2004; Pfefferbaum et al., 1985), known to elicit robust enhancement of the N2 and anterior-central P3 ERP components on 'nogo' trials relative to 'go' trials. Substantial 'go-nogo' modulation of the anterior-central P3 at single-subject level was measured concurrently with fMRI by Bregadze and Lavric (2006). Here we examined in a group of subjects the 'go' vs. 'nogo' difference in the amplitude of the N2 and P3 components in response to stimuli presented either during gradients or in the no-gradient gaps. To facilitate generalisation, we applied

widely used EEG-fMRI combined acquisition and artifact correction procedures, a standard whole-brain EPI scanning sequence, and standard segmentation and analysis of ERP components. We complemented the conventional ERP analysis with analyses based on single trials, aimed at assessing potential differences in the (experimental, 'go' vs. 'nogo') contrast-to-noise ratio between EEG stretches obtained in the gradients and in the no-gradient gaps, which could be undetected in ERP averages.

A further aspect that was investigated in the present study was the role of signal decomposition in the extraction of ERP components. Because EEG is a complex mixture of signals of cerebral and non-cerebral origin, statistical identification and separation of ERP components has been a central challenge in the ERP field. The most widely employed statistical procedures are Principal Components Analysis (PCA, Donchin and Heffley, 1976; Lavric et al., 2008; Weber and Lavric, 2008; Wills et al., 2007) and Independent Component Analysis (ICA, Bell and Sejnovski, 1995; Makeig et al., 1997).

ICA has been extensively used in EEG-fMRI studies for (pulse, ocular and movement-related) artifact correction either alone (e.g. Mantini et al., 2009) or in combination with other procedures (Debener et al., 2008; Eichele et al., 2005; Strobel et al., 2008). Since the aim of ICA is essentially the determination of spatial filters corresponding to maximally independent component signals, it has significant potential for the identification and separation of ERP components, which tend to have characteristic scalp distributions. Indeed, Debener et al. (2005) used ICA to identify the Error-Related Negativity in a combined EEG-fMRI paradigm and correlated its amplitude over single trials with the fMRI signal. ICA-based decomposition has the potential to improve the detection of prediction-based experimental modulations in ERP

components for at least three reasons: (1) it is likely to separate ERP components from artifacts; (2) because it results in the cancellation of artifact-related signal, rather than the removal of data-stretches containing artifact, ICA makes more data are available for analysis, improving the SNR; (3) it may disentangle (un-mix) temporally overlapping ERP components with different topographies. In the present investigation, we examine these expectations by performing all the analyses both with and without ICA-based decomposition.

To summarise, the aim of the present investigation is two-fold. First, we examine EEG measurement in-between sparse fMRI acquisition. Second, we assess the extraction of ERP components from EEG acquired in the scanner by means of ICA decomposition. The benefits of both procedures are evaluated in the context of detecting experimental (cognitive) modulations of long-latency ERP components in the 'go-nogo' paradigm.

METHODS

Participants

Ten right-handed participants (all female, mean age 24, range 18 – 39), provided informed written consent to participate in the study, whose procedure was approved by the local ethics committee. Participants were paid £20-25 (depending on duration) for their participation in the two testing sessions. The data from one participant was discarded due to failure to comply with task instructions.

Task, procedure and experimental manipulation

The study employed a 'go-nogo' task that required a right-hand button-press in response to the presentation of 'go' stimuli (probability 0.75) and withholding the response to 'nogo' stimuli (probability 0.25). Each condition used two letters in upper-/lowercase (go: B /b, J /j; nogo: P/p, G/g) presented centrally in white against a black background. The selection of condition/letter/case on each trial was random with the constraint that the two letters within each condition were equiprobable, as were upper-/lowercase presentations. Each participant was tested in two separate sessions (whose order was alternated over participants) about 1-3 days apart, and each session contained 464 trials. In one EEG session stimulus presentation was restricted to the 2 s fMRI volume acquisition (henceforth: 'gradient'), while in the other session stimuli were always presented in the 2 s gaps between fMRI volumes (henceforth: 'no-gradient'). To ensure a 700 ms stretch of EEG for ERP segmentation after each stimulus (600 ms post-stimulus onset plus 100 ms baseline), one stimulus per volume/gap was presented. In other words, in each of the two sessions, the temporal position of the -100 to 600 ms EEG segment, time-locked to the onset of the stimulus, was restricted to a time-window of 2 s, with one such segment acquired roughly every 4 s. The 600 ms segment post-stimulus onset was deemed sufficient for measuring the amplitude of the N2 and anterior P3 peaks in the ERP (N2 tends to reach maximum at 250-350 ms and anterior-central P3 at 350-550 ms). The stimulus, preceded by a 750 ms fixation cross, remained on the screen for the entire extent of the ERP epoch of 600 ms, after which it was replaced by a blank screen.

The precise timing of the ERP segment (dictated by the stimulus onset) was systematically jittered from trial to trial, by moving the onset of the stimulus relative to the onset of the 2 s time-window in 10 steps of 100 ms. On the first step, the stimulus was presented 200 ms into the time-window (200 ms into the gradient period or the no-gradient gap), allowing for a 100 pre-stimulus baseline to fit inside the 2 s time-window. The next stimulus was presented 300 ms into the time-window and so on; on the last jittering step the stimulus was presented 1100 ms into the time-window, allowing for a 600 ms of the post-stimulus ERP to fit in the 2 s time-window. The aim of jittering the position of the ERP segment within the gradient period or the no-gradient gap was to orthogonalize the timing of the ERP components relative to the timing of the gradient artifact. A stable temporal relationship between the two would mean that the averaging-based method used for gradient correction (see below) would subtract the ERP as well. The above temporal jittering was also done in the no-gradient session, because gradient correction in the no-gradient session had to be applied over the entire gradient & gap stretch. Although in that session ERPs were outside gradient-contaminated stretches, pulse artifact crossed the gradient-gap boundaries and the removal of gradient artifact only from part of the pulse artifact would distort (create discontinuities in) individual episodes of the ECG trace (reducing the effectiveness of their subsequent automatic detection) and individual episodes of the pulse artifact in the EEG channels (compromising the correction by sliding average, see below for details on the removal of pulse artefact).

EEG acquisition and artifact removal

The 32-channel EEG was acquired with a sampling rate of 5 kHz a bandpass of 0.016-250 Hz, the reference at FCz and the ground at FPz, using plastic-coated Ag/AgCl electrodes inserted in an elastic cap and a BrainAmp-MR amplifier (BrainProducts, Munich, Germany) connected to a PC outside the scanner room via a fibre-optic cable. 30 electrodes were placed on the scalp in an extended 10-20 configuration, one was placed below the right eye to record the vertical EOG and one at the medial end of the left collar bone to record the ECG.

The EEG was corrected for gradient and pulse artifacts using averaging-based procedures proposed by Allen et al. (2000) and Allen et al. (1998), respectively, both implemented in the BrainAnalyzer 1.05 software (BrainProducts, Munich, Germany). Stretches of EEG time-locked to markers of fMRI volume acquisition onset (which reliably indicated the onset of gradient artifact), were segmented, baseline-corrected to the mean amplitude across the stretch and averaged to create the template gradient artifact, which was subtracted from individual stretches of gradient artifact. The length of EEG stretches used for correction was 4 s- the interval between fMRI volumes (TR). In all but three participants, the average of all gradient stretches of the session was used to create the gradient artifact template. In the remaining participants gradient artifacts varied in amplitude throughout the session, probably due to head movement during the session, so a sliding average of 50 segments was used to form the template. There was no hardware synchronization of the scanner and EEG amplifier clocks (e.g. Anami et al., 2003; Mandelkow et al., 2006).

Following the removal of gradient artifact, the EEG was low-pass filtered at 50 Hz and downsampled by a factor of 20 (to 250 Hz). For pulse artifact correction, heartbeats were identified in the ECG channel by an automated procedure, which searched through the first 20 seconds of a sliding standard deviation window for ranges, in which the standard deviation of the ECG rose suddenly as an indication of the start of a heartbeat episode. The detected episodes were averaged to form the ECG template. Subsequently, an algorithm searched the ECG time-point by time-point for stretches of data of the same length as the template that matched the template. There were two constraints: (1) minimum interval between matches ≥ template length; (2) maximum interval=1.5 s, corresponding to a minimum heart-rate of 40 bpm. There were two criteria for a match: cross-correlation and amplitude similarity. The latter was computed as the average of template/data ratios of amplitudes at each time-point (prior to ratios being computed, amplitudes were demeaned to minimise the impact of baseline shifts or trends). The points of the best matches of the data to the template were marked if cross-correlation was at least 0.7 and the amplitude similarity between 0.7 and 1.2. The stretches that were best matches but were below these values were also marked and later verified/confirmed by visual inspection.

To mark the onset of the pulse artifact in the EEG, one has to estimate the time-delay between the markers of heartbeats in the ECG and the onset of the pulse artifact in the scalp EEG. This estimation was done using Global Field Power (GFP) calculations. First, GFP and power in individual channels were calculated and then averaged for 3 s-long EEG stretches time-locked (-1 s to 2 s) to the markers in the ECG channel. Subsequently, channels whose summed power (over time) in these stretches exceeded a

threshold = GFP/nr channels were selected and GFP was re-calculated for the same stretches only based on the selected channels. The GFP maximum following the ECG marker was then identified, as were the GFP minima that immediately preceded and followed the maximum. The interval between the mid-point between these minima and the ECG marker was used as the time-delay between the ECG markers and the onset of the pulse artifacts in the scalp EEG, and markers were set in the EEG accordingly. EEG segments time-locked to these markers were corrected using a sliding average subtraction (with 21 segments in the sliding window).

EEG/ERP analysis

Following gradient and pulse artefact correction and prior to ERP segmentation the EEG was processed in two ways: without signal decomposition (henceforth referred to as 'no-ICA analysis') and with signal decomposition (henceforth: 'ICA-based analysis'). The ICA-based analysis comprised three extra steps: (1) running Infomax ICA (Bell and Sejnovski, 1995; Makeig et al., 1997; implemented in the Brain Analyzer software) on the continuous EEG data in all the scalp channels for each subject and session (gradient and no-gradient); (2) selecting, for every subject and session the ICA components with a topography consistent with the central (FCz-Cz) scalp distribution of the go-nogo N2 and P3 effects and a time-course containing peak(s) in the N2 and/or P3 range (mean number of components selected in a data-set, 1.8; standard deviation, 1; maximum, 4); (3) back-transforming the selected components into the EEG channel space.

The subsequent processing stages were equivalent in the no-ICA and ICA-based analyses, except that in the no-ICA analysis an automated procedure marked the onsets and offsets of eyeblinks and ERP segments containing these were later discarded in the segmentation stage (these segments were not removed in the ICA-based analysis). Prior to segmentation, the EEG was re-referenced to the average reference and mastoid channels were excluded from the reference and further analysis, because they are particularly prone to cardioballistic artifacts due to the proximity to the temporal artery. We obtained EEG segments time-locked to 'go' stimuli (-100 to 600 ms), to which a response was made, and 'nogo' stimuli that were not followed by (inappropriate) responses. A small number of EEG segments were discarded in both analyses (with and without ICA) due to movement-related artifact or large signal drifts. In the no-ICA analysis, the rejection of segments contaminated by ocular artifact left in the gradient session an average of 293 'go' segments (standard deviation, 45.4) and 83.9 'nogo' segments (standard deviation, 19); in the no-gradient session there were 276.9 'go' segments (standard deviation, 63.4) and 85.4 'nogo' segments (standard deviation, 18.8). In the ICA-based analysis (in which more trials were retained because segments containing eyeblinks were not discarded) there were on average 340.4 'go' segments (standard deviation, 9.2) and 109 'nogo' segments (standard deviation, 3.9) in the gradient session and 340.2 'go' segments (standard deviation, 4.3) and 107.9 'nogo' segments (standard deviation, 5.5) in the no-gradient session. Following segmentation and baseline (-100 - 0 ms) correction, the EEG data were submitted to: (1) a conventional ERP amplitude analysis (based on averages of the 'go' and 'nogo' segments); (2) an amplitude analysis based on single-trial EEG data, and (3) a reliability analysis. The first

two analyses focused on the detection of the experimental (go-nogo) effects in the ERP ranges under scrutiny (N2, P3), whereas the third analysis was concerned with the correspondence between these components in the gradient and no-gradient data.

(1) For the conventional ERP amplitude analysis, the amplitude of the N2 and the anterior-central P3 components was measured as the voltage averaged within 100-ms time-windows centred on the N2 and anterior-central P3 peaks in the grand-average ERP. Given the well-documented central scalp distribution of these components in the go-nogo paradigm, two electrodes were selected for the analysis: FCz and Cz. ANOVAs with factors condition (go vs. nogo), gradient (present vs. absent), ICA (with vs. without) and electrode (FCz vs. Cz) along with paired t tests were used to examine N2 and P3 amplitude.

(2) In addition to the amplitude analyses based on averaged segments, we examined the detectability of the go-nogo effects in single subjects using single-trial EEG. The single-subject analyses were run on both data that were/were not subjected to ICA-based decomposition. We used the independent samples t statistic in individual subjects, with single trial EEG/ERP amplitudes as observations. As in the above ERP analyses, single trial amplitudes were averaged in 100-ms time-windows. The time-windows were determined in each subject individually from the timing of the relevant peak (N2 or P3) in the subject's average ERP. For both components, the Cz electrode was subjected to analysis. Given the relatively large number of tests (9 per contrast) and the associated

inflation of type 1 error, the significance level was Bonferroni-corrected for each contrast.

(3) To assess the correspondence between the EEG/ERP data in the gradient and no-gradient sessions and the potential benefit of ICA decomposition, reliability analyses were performed for the N2 and anterior-central P3 components. Pearson's correlation (r) was used as a relative measure of reliability and intraclass correlation (Cronbach's α) as an absolute measure of reliability; both correlations were computed over subjects. First, we examined the session-to-session (gradient - no-gradient) reliability of subjects' go-nogo differences and of the single-subject t statistic values obtained in analysis (2) above. Second, to compare the within-session measurement error in the gradient and no-gradient sessions, Pearson's r and Cronbach's α were used to compute 'split-half reliability'- a measure of consistency of mean ERP amplitude computed separately for trials with odd numbers and trials with even numbers (in temporal order). This evaluation of measurement error was done for:

- the ERP amplitude in the N2 and P3 range, irrespective (collapsed over) the go-nogo factor. To ensure the same 'go'/'nogo' ratio in the 'odd' and 'even' means, these means were initially computed separately for 'go' and 'nogo' conditions and then the two conditions were averaged within each split-half.
- the go-nogo difference in the N2 and P3 range.

Because reliability calculations in the ICA-based analysis were based on ~20% more trials than in the no-ICA analysis, we adjusted (downwards) the reliability

coefficients in the ICA-based analysis using the Spearman-Brown prophecy formula (unadjusted and adjusted values are reported).

fMRI Parameters

Although the study was restricted to ERP analyses, we outline the fMRI acquisition parameters because they largely determine the characteristics the MR-related artifact in the EEG: EPI sequence, run in a 1.5 T Philips Gyroscan scanner; TR 4000 ms; TE 40 ms; TA (volume acquisition time) 1980 ms (2020 ms gradient free per TR); flip angle 90°; FOV: 230×230 mm; 64×64 within-plane matrix; 22 contiguous transverse slices 4 mm thick with a 2 mm gap.

RESULTS

Performance accuracy was high (above 93%) in all subjects in both experimental conditions. The inspection of the ERPs revealed similar waveforms and, importantly, 'go' vs. 'nogo' effects, in the gradient and no-gradient sessions, with and without ICA decomposition (Fig. 1). The N2 and anterior-central P3 had greater amplitude in the 'nogo' condition in both the gradient and no-gradient ERPs. Global Field Power in the average ERPs was also quite similar in the two sessions (Fig. 2). The inspection of the scalp distribution of the go-nogo differences showed that, although the N2 peak was

restricted to the central electrodes and no clear N2 peak could be seen in electrodes posterior to Cz, the go-nogo negativity in the N2 range had a parietal maximum in the no-ICA analysis, with or without gradients (Fig. 3, top left panel). Careful inspection of the parietal electrode Pz in Figure 1 indicates that this was due to a delayed parietal P3 (P3b) in the 'nogo' condition relative to the 'go' condition. Because in the data subjected to ICA-based decomposition only the components with central distribution were selected, one would expect the ICA-based analysis of N2 to reduce the effects on posterior P3. This was indeed the case: following ICA decomposition, the amplitude of P3b was strongly attenuated (relative to the no-ICA analysis) (Fig. 1, right), as was the contribution of the P3b latency shift to the topography of the N2 go-nogo effect (Fig. 3, top right).

Conventional ERP amplitude analysis

N2. The ANOVA on the averaged amplitude within the 100-ms window (260-360 ms) centred on the N2 peak (~310 ms, Fig. 1) found a marginally significant main effect of condition (more negative amplitudes for 'nogo', $F(1,8) = 4.7$, $p = 0.06$) and a significant interaction between ICA and electrode ($F(1,8) = 8.87$, $p = 0.018$), reflecting a more central distribution of the ERPs in the ICA-based analysis. Neither the main effect of gradient ($F(1,8) = 0.14$, $p = 0.91$), nor its interaction with condition ($F(1,8) = 0.14$, $p = 0.907$) approached significance. In the no-ICA analysis, the N2 amplification on 'nogo' trials was significant for electrode Cz in the gradient session, but failed to reach

significance in the no-gradient session for either FCz or Cz (Table 1). In the ICA-based analysis, a significant N2 modulation was found for FCz in both gradient and no-gradient ERPs; whereas for Cz the contrasts were significant only as one-tailed.

P3. The anterior-central P3 peaked at about 500 ms after the stimulus onset (Fig. 1) and was analysed in a 100 ms time-window centred on 500 ms (450-550 ms). The ANOVA revealed a significant effect of condition ($F(1,8) = 19.69$, $p = 0.002$), reflecting greater P3 amplitude on 'nogo' trials, and a significant ICA by electrode interaction ($F(1,8) = 8.87$, $p = 0.018$), suggestive of a slightly more anterior scalp distribution of the ERPs in this window in the ICA-based analysis in both 'go' and 'nogo' ERPs (Fig. 1). As with N2, neither the main effect of gradient, nor its interaction with condition was significant ($Fs < 0.7$, $ps > 0.5$). Follow-up t-tests (Table 1) in the no-ICA analysis revealed significant a 'go-nogo' difference in the gradient ERPs for electrode FCz; for Cz this difference was only significant as one-tailed. In the no-gradient data, the difference was significant for both electrodes. In the ICA-based analysis, the P3 effect was significant in both sessions and for both electrodes.

Single-trial analyses

N2. The procedure employed at this stage of the analysis was based on the independent samples t statistic run for each subject with single-trials as observations (see Methods). In the no-ICA analysis, 8 subjects showed a greater 'nogo' N2 in the gradient session (4

significantly so) and 6 in the no-gradient session (2 significantly so) (Table 2). The mean t statistic for the N2 effect was greater in the gradient session than in the no-gradient session (2.23 vs. 0.98), though not significantly so, as indicated by a paired-samples t test on individual subjects' t values ($t(8) = 1.78$, $p = 0.11$). In the ICA-based analysis, 8 subjects had the expected 'nogo' vs. 'go' N2 negativity in the gradient session and 7 in the no-gradient session (4 and 3 were significant, respectively). The mean single-subject t values for the two sessions (gradient, 2.45; no-gradient, 2.35) were not statistically distinguishable from one another. Although the mean subject-wise t values were greater in the ICA-based analysis than in the no-ICA analysis (see above), an ANOVA with factors ICA and gradient found a main effect of ICA that did not reach significance ($F(1,8) = 2.18$, $p = 0.18$). Nevertheless, there was a trend in the interaction between factors ICA and gradient ($F(1,8) = 4.25$, $p = 0.073$), followed by a greater subject-wise mean t statistic in the ICA-based analysis than in the no-ICA analysis for the no-gradient session ($t(8) = 3.51$, $p = 0.008$).

P3. The P3 no-ICA analysis over single trials revealed that 8 subjects showed the expected 'nogo'-P3 enhancement in each session (with or without gradients); it was significant in 5 subjects in each session (Table 3). The mean t statistic was greater in the in the 'no gradients' session relative to the 'gradients' session (-3.29 vs. -2.21), but not significantly so ($t(8) = 1.39$, $p = 0.2$). In the ICA-based analysis, all 9 subjects showed a 'nogo'-P3 enhancement in the gradient session (5 significantly so) and 8 subjects in the no-gradient session (6 significantly so). The mean t statistic was greater in the no-gradient (-5.07) than in the gradient (-3.67) session, but this difference did not reach

significance (t(8) = 1.86, p = 0.1). As it was the case with N2, individual subjects' t-values were larger following ICA-based decomposition than in the no-ICA analysis (see above). However, the main effect of ICA in did not reach significance in the ICA by gradient ANOVA (F(1,8)=2.98, p=0.12), nor did the ICA by gradient interaction (F(1,8)=0.21, p=0.66).

Reliability analyses

Cross-session (gradient – no-gradient) reliability: N2. To assess the degree of correspondence between the go-nogo effects observed in the gradient and no-gradient sessions, correlations were computed over subjects for the go-nogo differences and the individual subjects' t statistic in the two sessions. In the no-ICA analysis, the Pearson correlations were r(9) = 0.59, p = 0.092 (go-nogo difference) and r(9) = 0.42, p = 0.26 (individual subjects' t), and the intraclass correlations were 0.7 (go-nogo difference) and 0.55 (individual subjects' t). All correlations were higher in the ICA-based analysis: Pearson, r(9) = 0.7 (0.65[1]), p = 0.035 (go-nogo difference); r(9) = 0.78 (0.74), p = 0.013 (individual subjects' t); intraclass, 0.88 (0.85) (go-nogo difference) and 0.81 (0.77) (individual subjects' t).

Cross-session (gradient – no-gradient) reliability: P3. The correlations between the gradient and no-gradient sessions in the no-ICA analysis were: Pearson's r(9) = 0.68, p =

[1] The value in parentheses was adjusted downwards corresponding to 20% fewer trials using the Spearman-Brown prophecy formula, see Methods.

0.045 (go-nogo difference); r(9) = 0.73, p = 0.025 (individual subjects' t); intraclass, 0.8 (go-nogo difference) and 0.84 (individual subjects' t). All correlations were higher in the ICA-based analysis: Pearson, r(9) = 0.95 (0.94), p < 0.001 (go-nogo differences); r(9) = 0.8 (0.76), p = 0.011 (individual subjects' t); intraclass, 0.97 (0.96) (go-nogo differences) and 0.86 (0.83) (individual subjects' t).

Split-half reliability. To assess the measurement error, split-half (odd-even) correlations were computed for each session for the ERP amplitude (averaged in the 100-ms windows used in the single-trial analysis above), as well as for go-nogo difference in the same windows (Tables 4 and 5). In the no-ICA analysis, these correlations were substantial for the ERP amplitude, but lower for the go-nogo difference. Pearson's and the intraclass correlations were higher for the no-gradient session in the N2 analysis, however, this reversed in the P3 analysis, where both correlations were higher in the gradient session.

In the data that were subjected to ICA-based decomposition, all correlations were much higher than in the no-ICA data. The difference between the ICA-based and no-ICA analyses was particularly striking in the correlations run on the go-nogo differences, indicating a very substantial reduction (relative to the no-ICA analysis) in the measurement error of the go-nogo differential effects. This was the case for both sessions (gradient, no-grdient) and both ERP components under scrutiny (Tables 4 and 5).

DISCUSSION

A commonly employed strategy for eliminating the effects of gradient switching artifact in combined ERP-fMRI studies is to use of sparse fMRI and present the stimuli in intervals during which no fMRI acquisition takes place (Debener et al., 2005; Eichele et al., 2005; Liebenthal et al., 2003; Mulert et al., 2004; Strobel et al., 2008). However, the sparse positioning of ERP stimuli (and fMRI scans) restricts the number of stimuli (and the amount of data), constrains their timing and leaves some portions of the BOLD fMRI signal time-course systematically under-sampled. An important issue is, therefore, whether there are clear benefits of interleaving ERPs and fMRI. Studies that examined the effect of gradient artifacts on visual evoked potentials, found no such benefits; they reported similar amplitudes and latencies of the P1-N1 complex acquired during vs. outside gradient intervals (Becker et al., 2005; Warbrick and Bagshaw, 2008). Nevertheless, the effect of gradients on the detection of more subtle, experimentally-induced, changes in the ERPs has not been examined yet, particularly for longer latency ERP components associated with stimulus categorisation, or conflict and performance monitoring (e.g. N2, P3, Error-Related Negativity).

The main objective of the current study was to establish whether ERP acquisition in gaps containing no gradient artifact leads to superior detection of experimentally-induced effects in two ERP components. We employed a well-documented paradigm known to elicit robust modulations of ERP components- the 'go-nogo' paradigm (Eimer, 1993; Falkenstein et al., 1999; Lavric et al., 2004; Pfefferbaum et al., 1985). It is important to make it clear that we exploited the modulation of N2 and anterior-central P3 in a 'proof-of-concept' approach, without aiming to resolve the controversies in the interpretation of the N2 (e.g. Falkenstein et al., 1999; Nieuwenhuis et al., 2003) or the

'nogo'-P3 amplification (e.g. Salisbury et al., 2001). In statistical terms, we set the goal of assessing whether the experimental contrast ('go' vs. 'nogo')-to-noise ratio was greater in the ERPs acquired in the absence of concurrent MR gradient switching than in the ERPs acquired with concurrent gradient switching, both in averaged ERPs and over individual EEG segments. The latter analysis was motivated by the increasingly popular approach of correlating ERP component amplitude (or latency) with the fMRI signal over single trials (see Debener et al., 2006, for a review).

Effects of gradient artifact

The ERP components under scrutiny (N2 and anterior-central P3) were clear in the averaged ERPs (Fig. 1). In the conventional ERP analysis (based on averaged trials) the magnitude of the 'go-nogo' difference, as well as the overall size of the N2 and P3 peaks, was statistically indistinguishable across the two sessions in the averaged ERPs. Weak (non-significant) trends suggested that the modulation of the N2 amplitude was somewhat better detected in the 'gradient' ERPs, whereas the P3 modulation seemed slightly more detectable in the 'no-gradient' ERPs (Table 1). The analyses based on single trials were largely consistent with the above results. For both N2 and P3, the vast majority of participants showed effects in the predicted direction in t tests run within individuals (Tables 2 & 3). These effects were more robust for the P3 component, for which most participants showed statistically significant amplitude enhancement in 'nogo' trials (in both the 'gradient' and 'no gradient' ERPs); for N2, a third to half of the

participants showed statistically significant amplitude enhancement in ‘nogo’ trials. The t statistic computed in individual subjects was not significantly different in the gradient vs. no-gradient sessions.

The analysis aimed at examining the measurement error (split-half reliability) found, as one would expect, higher split-half reliability for the ERP amplitude (collapsed across conditions) than for the ‘go-nogo’ difference (Tables 4 & 5). There were no systematic differences in the reliability measures between the gradient and no-gradient sessions. Whilst the coefficients for the ‘go-nogo’ N2 difference were greater for the no-gradient session than for the gradient session, this reversed for the P3 component.

Finally, the correspondence between the ‘go-nogo’ effects in the gradient and no-gradient sessions, as assessed by means cross-session reliability measures, was good, particularly if one takes into account the relatively small sample size (9). Even without ICA decomposition, three out of four Pearson coefficients were above 0.5 and three out of four Cronbach coefficients were above 0.7.

Effects of ICA-based decomposition

Another objective of the present study was to examine the potential benefits of signal decomposition in the extraction of ERP components. Rather than using signal-decomposition solely for artifact cancellation, we employed ICA (Bell and Sejnovski, 1995) for the selection of component signals that had the predicted topography and time-course (cf. Debener et al., 2005). There are good reasons to expect ICA-based

decomposition and selection to result in superior detection of experimentally-driven ERP modulations (see Introduction). Our analyses confirmed these expectations.

First, ICA-based decomposition resulted in better validity in the identification of the predicted (typical) scalp distribution of the 'go-nogo' difference in the N2 component. In the no-ICA analysis, the expected amplitude difference between the 'go' and 'nogo' ERPs at the FCz and Cz electrode locations was largely overshadowed by a more posterior difference (Fig. 3) resulting from the latency shift in the parietal P3 (P3b) component (electrode Pz in Fig. 1). The selection of N2-related ICA components strongly attenuated the contribution of P3b and its latency shift, hence the typical topography of the 'go-nogo' N2 difference could be clearly recovered (Fig. 3). Second, greater cross-session reliability coefficients in the ICA-based analysis indicate better stability of the detected experimental modulations relative to the analysis without ICA, which is also noticeable in single-trial overlay plots (Fig. 4). Third, the split-half reliability analysis points to much lower measurement error in the ICA-based analysis for both ERP components under examination, particularly in the detection of the differential ('go' vs. 'nogo') effect (Tables 4 & 5). Fourth, the analysis of the magnitude of the 'go-nogo' difference also points to some benefit of applying ICA-based decomposition, although the difference in the magnitude of the detected effect was statistically significant only in the comparison of individual subjects' t statistic for N2 in the no-gradient session.

Conclusions

We found little evidence of a benefit of 'fast interleaved' ERP-fMRI acquisition (see Introduction) for the measurement of experimentally-induced ERP effects. While there were some differences in the detectability of N2 and P3 modulations between the ERPs acquired during MR gradient switching or in its absence, their direction was not systematic and they were statistically weak. Although it is possible that there may be a benefit associated with acquiring ERPs outside the gradients, which escaped detection, we would argue that such a benefit is small and unlikely to outweigh the costs of acquiring less data with sub-optimal stimulus presentation and sampling of the BOLD response. We also note that our conclusion is not based exclusively on the null effect of failing to reveal significant differences between the gradient and no gradient ERPs, but also on positive evidence of statistically significant ERP differences in the gradient ERPs for both N2 and anterior-central P3. Because the present investigation is concerned with ERPs, the above conclusion may not apply to other EEG analyses, in particular, to those of experimentally-induced frequency modulations. However, recent work on the optimisation of average-based gradient correction in combination with scanner-EEG amplifier phase synchronisation and fMRI sequence optimisation, shows that even very subtle ultra-fast EEG frequency bursts can be recovered from gradient-contaminated data (Freyer et al., 2009).

It is reasonable to consider whether the use of alternative artifact correction techniques may have led to a different conclusion. For instance, one may ask whether other (superior) pulse artifact correction might have revealed effects of gradients that our analyses missed. The present results contain a tentative answer to this question. Because in the ICA-based analysis only ICA components with the desired characteristics were

selected (which left out components that captured pulse artifact), ICA selection was, in effect, an additional stage of pulse artifact correction. Although the ICA-based analysis resulted in an overall improvement in the detection of the expected ERP modulations, it did not reveal substantially greater differences between the gradient and no-gradient sessions.

Our conclusion concerning the role of ICA-based decomposition in the extraction of ERPs is that there are marked benefits in employing such decomposition when one seeks to isolate ERP effects with a known topography. While similar considerations apply to ERPs acquired outside the MR environment, the presence of extra artifacts makes procedures such as ICA particularly useful for ERP component extraction in combined EEG-fMRI.

References

Allen PJ, Josephs O, Turner R. A method for removing imaging artifact from continuous EEG recorded during functional MRI. Neuroimage 2000;12:230-9.

Allen AJ, Polizzi G, Krakow K, Fish D, Lemieux L. Identification of EEG events in the MR scanner: the problem of pulse artifact and a method for its subtraction. Neuroimage 1998;8:229-39.

Anami K, Mori T, Tanaka F, Kawagoe Y, Okamoto J, Yarita M, Ohnishi T, Yumoto M, Matsuda H, Saitoh O. 2003. Stepping stone sampling for retrieving artifact-free electroencephalogram during functional magnetic resonance imaging. Neuroimage 2003;19:281-95.

Becker R, Ritter P, Moosmann M, Villringer A.. Visual evoked potentials recovered from fMRI scan periods. Hum Brain Mapp 2005;26:221–30.

Bell AJ, Sejnowski TJ. An information-maximization approach to blind separation and blind deconvolution. Neural Comput 1995;7:1129-59.

Bénar C-G, Schön D, Grimault S, Nazarian B, Burle B, Roth M, Badier J-M, Marquis P, Liegeois-Chauvel C, Anton J-C. Single-trial analysis of oddball eventrelated potentials in simultaneous EEG-fMRI. Hum Bain Mapp 2007;28:602–13.

Bonmassar G, Schwartz DP, Liu AK, Kwong KK, Dale AM, Belliveau JW. Spatiotemporal brain imaging of visual-evoked activity using interleaved EEG and fMRI recordings. Neuroimage 2001;13:1035-43.

Bregadze N, Lavric A. ERP differences with vs. without concurrent fMRI. Int J Psychophysiol 2006;62:54-9.

Comi E, Annovazzi P, Silva AM, Cursi M, Blasi V, Cadioli M, Inuggi A, Falini A, Comi G, Leocani L. Visual evoked potentials may be recorded simultaneously with fMRI scanning: A validation study. Hum Brain Mapp 2005;24:291-8.

Debener S, Ullsperger M, Siegel M, Fieler K, Von Cramon DY, Engel A. Trial-by-trial coupling of concurrent electroencephalogram and functional magnetic resonance Imaging identifies the dynamics of performance monitoring. J Neurosci 2005; 25:11730-7.

Debener S, Ullsperger M, Siegel M, Engel A. Single-trial EEG–fMRI reveals the dynamics of cognitive function. Trends Cogn Sci 2006;10:558-63.

Debener S, Mullinger KJ, Niazy RK, Bowtell RW. Properties of the ballistocardiogram artifact as revealed by EEG recordings at 1.5, 3 and 7 Testla static magnetic field strength. Int J Psychophysiol 2008;67:189-99.

Eichele T, Specht K, Moosmann M, Jongsma MLA, Quirogal RQ, Nordby H, Kenneth H. Assessing the spatiotemporal evolution of neuronal activation with single-trial event-related potentials and functional MRI. Proc Natl Acad Sci 2005; 102:17798-803.

Eimer M. Effects of attention and stimulus probability on ERPs in a Go/Nogo task. Biol Psychol 1993;35:123-38.

Falkenstein M, Hoormann J, Hohnsbein J. ERP components in Go/Nogo tasks and their relation to inhibition. Acta Psychol 1999;101:267-91.

Freyer F, Becker R, Anami K, Curio G, Villringer A, Ritter P. Ultrahigh-frequency EEG during fMRI: Pushing the limits of imaging-artifact correction. Neuroimage 2009;48:94-108

Laufs H, Daunizeau J, Carmichael DW, Kleinschmidt A. Recent advances in recording electrophysiological data simultaneously with magnetic resonance imaging. Neuroimage 2008;40:515-28.

Lavric A, Mizon GA, Monsell S. Neurophysiological signature of effective anticipatory task-set control: a task-switching investigation. Eur J Neurosci 2008;28:1016-29.

Lavric A, Pizzagalli D, Forstmeier S. When ‘go’ and ‘nogo’ are equally frequent: ERP components and cortical tomography. Eur J Neurosci 2004;20:2483-8.

Liebenthal E, Ellingson LM, Spanaki MV, Prieto TE, Ropella KM, Binder JR. Simultaneous ERP and fMRI of the auditory cortex in a passive oddball paradigm, Neuroimage 2003;19:1395-404.

Makeig S, Bell AJ, Jung T-P, Ghahremani D, Sejnowski TJ. Blind separation of auditory event-related brain responses into independent components. Proc Natl Acad Sci USA 1997;94:10979-84.

Mandelkow H, Halder P, Boesiger P, Brandeis D. Synchronization facilitates removal of MRI artifacts from concurrent EEG recordings and increases usable bandwidth. Neuroimage 2006;32:1120-6.

Mantini D, Corbetta M, Perrucci MG, Romani GL, Del Gratta C. Large-scale brain networks account for sustained and transient activity during target detection. Neuroimage 2009;44:265-74.

Mulert C, Jäger L, Schmitt R, Bussfeld P, Pogarell O, Möller HJ, Juckel G, Hegerl U. Integration of fMRI and simultaneous EEG: towards a comprehensive understanding of localization and time-course of brain activity in target detection. Neuroimage 2004;22: 83-94.

Mullinger K, Debener S, Coxon R, Bowtell R. Effects of simultaneous EEG recording on MRI quality at 1.5, 3 and 7 Tesla. Int J Psychophysiol, 2008;67:178-188.

Niazy RK, Beckman CF, Iannetti GD, Brady JM, Smith SM. Removal of fMRI environmental artifacts from EEG data using optimal basis sets. Neuroimage 2005;28:720-37.

Nieuwenhuis S, Yeung N, van den Wildenberg W, Ridderinkhof KR. Electrophysiological correlates of anterior cingulate function in a Go/NoGo task: Effects of response conflict and trial-type frequency. Cogn Affect Behav Neurosci 2003;3:17-26.

Pfefferbaum A, Ford JM, Weller BJ, Kopell BS. ERPs to response production and inhibition. Electroencephalogr Clin Neurophysiol 1985;60:423-34.

Salisbury DF, Rutherford B, Shenton ME, McCarley, RW. Button-pressing affects P300 amplitude and scalp topography. Clin Neurophysiol 2001;112:1676-84.

Strobel A, Debener S, Sorger B, Peters JC, Kranczioch C, Hoechstetter K, Engel AK, Brocke B, Goebel R. Novelty and target processing during an auditory novelty oddball: a simultaneous event-related potential and functional magnetic resonance imaging study. Neuroimage 2008;40:869-83.

Warbrick T, Bagshaw AP. Scanning strategies for simultaneous EEG–fMRI evoked potential studies at 3 T. Int J Psychophysiol 2008;67:169-77.

Warbrick T, Mobascher A, Brinkmeyer J, Musso F, Richter N, Stoecker T, Fink GR, Shah NJ, Winterer G. Single-trial P3 amplitude and latency informed event-related fMRI models yield different BOLD response patterns to a target detection task. Neuroimage 2009;47:1532-44.

Weber K, Lavric A. Syntactic anomaly elicits a lexico-semantic (N400) ERP effect in the second but not in the first language. Psychophysiol 2008;45:920-5.

Wills A J, Lavric A, Croft G S, Hodgson T L. Predictive learning, prediction errors, and attention: evidence from event-related potentials and eye tracking. J Cogn Neurosci 2007;19:843-54.

Table 1. The results from t-tests run on subjects' averaged ERPs (conventional analysis).

Component	Electrode	No-ICA		ICA	
		Gradient	No gradient	Gradient	No gradient
N2	FCz	t=1.1, p=0.3	t=0.79, p=0.45	t=2.45, p=0.04*	t=2.34, p=0.048*
	Cz	t=2.64, p=0.03*	t=1.28, p=0.24	t=2.05, p=0.074	t=2.0, p=0.081
P3	FCz	t=4.5, p=0.002**	t=3.81, p=0.005**	t=3.61, p=0.007**	t=4.2, p=0.003**
	Cz	t=2.06, p=0.073	t=3.45, p=0.009**	t=2.47, p=0.039*	t=4.01, p=0.004**

df = 8;

* $p < 0.05$

** $p < 0.01$

Table 2. Independent samples go vs. nogo t-tests run in individual subjects on the mean amplitude within a 100-ms N2 time-window in single trial EEG data.

Subject	No-ICA		ICA	
	Gradient	No gradient	Gradient	No gradient
1	3.23*	3.23*	-0.44	2.70
2	2.46	4.77*	7.16*	7.08*
3	4.40*	1.76	2.66	2.62
4	1.17	-1.21	1.04	-0.87
5	2.73*	1.57	2.73*	3.10*
6	-0.85	0.41	0.66	1.90
7	2.10	-0.18	3.17*	3.41*
8	3.09*	1.08	3.17*	2.67
9	1.78	-2.60	1.86	-1.48

* $p < 0.05$ (Bonferroni-corrected)

Table 3. Independent samples go vs. nogo t-tests run in individual subjects on the mean amplitude within a 100-ms P3 time-window in single trial EEG data. The grey background indicates a significant effect in the opposite direction to the predicted effect.

Subject	No-ICA		ICA	
	Gradient	No gradient	Gradient	No gradient
1	-3.21*	-0.21	-7.85*	-8.88*
2	-3.75*	-4.06*	-6.33*	-7.67*
3	3.18*	0.99	-0.95	-1.76
4	-0.25	-4.32*	-2.02	-5.90*
5	-2.64	-5.71*	-3.86*	-6.96*
6	-0.42	-0.68	-1.41	-1.56
7	-2.87*	-1.11	-0.09	1.55
8	-2.78*	-4.83*	-6.71*	-5.54*
9	-7.11*	-9.69*	-3.84*	-8.96*

* $p < 0.05$ (Bonferroni-corrected)

Table 4. Split-half reliabilities (relative and intraclass correlations) for N2. For the ICA-based analysis, reliability adjusted for the number of trials using the Spearman-Brown prophecy formula is given in parentheses (some adjusted values are not different from the unadjusted ones due to the rounding error).

	Average ERP amplitude				Go-nogo difference			
	No-ICA analysis		ICA-based analysis		No-ICA analysis		ICA-based analysis	
	Grad	No grad	Grad	No grad	Grad	No grad	Grad	No grad
Pearson's r	0.87*	0.70*	0.99* (0.99*)	0.99* (0.99*)	0.32	0.43	0.81* (0.77*)	0.98* (0.98*)
Cronbach's α	0.91	0.80	0.99 (0.99)	0.99 (0.99)	0.40	0.59	0.89 (0.87)	0.99 (0.99)

* $p < 0.05$

Table 5. Split-half reliabilities (relative and intraclass correlations) for P3 (presentation as in Table 3).

	Average ERP amplitude				Go-nogo difference			
	No-ICA analysis		ICA-based analysis		No-ICA analysis		ICA-based analysis	
	Grad	No grad	Grad	No grad	Grad	No grad	Grad	No grad
Pearson's r	0.91*	0.92*	0.99* (0.99*)	0.99* (0.99*)	0.58	0.18	0.93* (0.91*)	0.86* (0.83*)
Cronbach's α	0.95	0.95	0.99 (0.99)	0.97 (0.96)	0.74	0.21	0.99 (0.99)	0.92 (0.90)

* $p < 0.05$

Figure legends:

Figure 1. Grand-average ERPs (over participants) at all midline electrodes. The greater N2 and anterior-central P3 peaks on 'nogo' trials can be clearly seen with/without gradients and ICA decomposition.

Figure 2. Global field power (computed as root-mean-square) of the ERPs for both conditions ('go', 'nogo') and both sessions (gradient, no-gradient) in the no-ICA analysis. Note the small differences (< 1μV) between the sessions in the ranges of N2 (260-360 ms) and anterior-central P3 (450-350 ms).

Figure 3. Spline-interpolated scalp distributions of the go-nogo difference for the N2 (260-360 ms) and P3 (450-350 ms) time windows. Despite the presence of a midline-central N2 effect (see electrodes FCz and Cz in Fig. 1), in the absence of ICA decomposition, the N2 difference topography is largely overshadowed by a latency shift in the posterior P3 (P3b; see also electrode Pz in the left panel of Fig. 1). The effect of P3b on the N2 topography is strongly attenuated in the ICA-based analysis: the N2 effect has its typical midline distribution in this analysis (see also electrode Pz in the right panel of Fig. 1).

Figure 4. Overlay plots of single-trial EEG data and the ERP superimposed in contrasting colour from four representative subjects. The scales (omitted in the interests of space economy) were equivalent within subjects for the two conditions ('go', 'nogo')

and sessions (gradient, no-gradient), but not for the ICA-based and no-ICA analyses; the scales were not equivalent for different subjects. The plots illustrate the greater cross-session (gradient, no-gradient) reliability in the ICA-based analysis.

Figure 1

Click here to download high resolution image

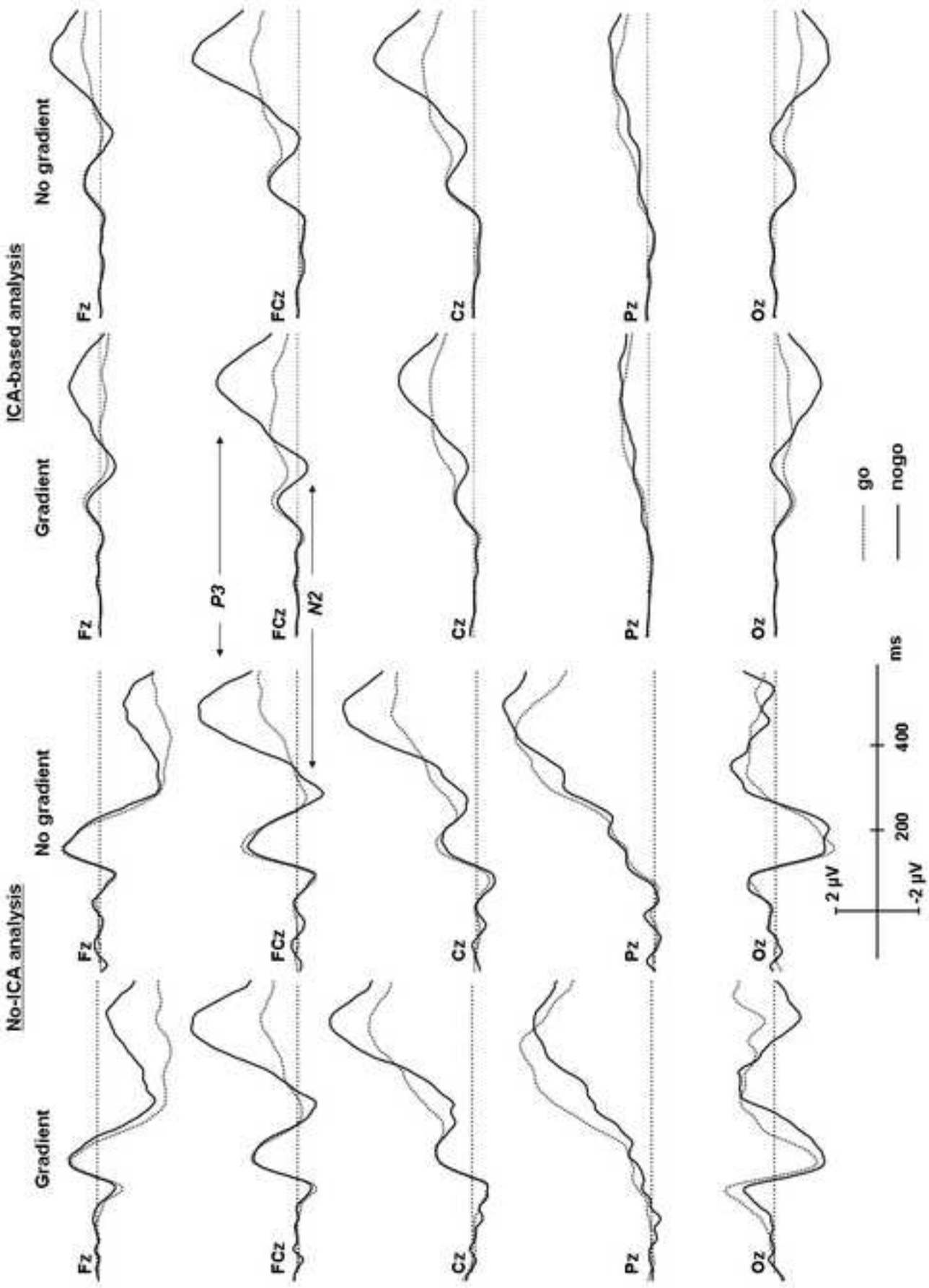

Figure 2
Click here to download high resolution image

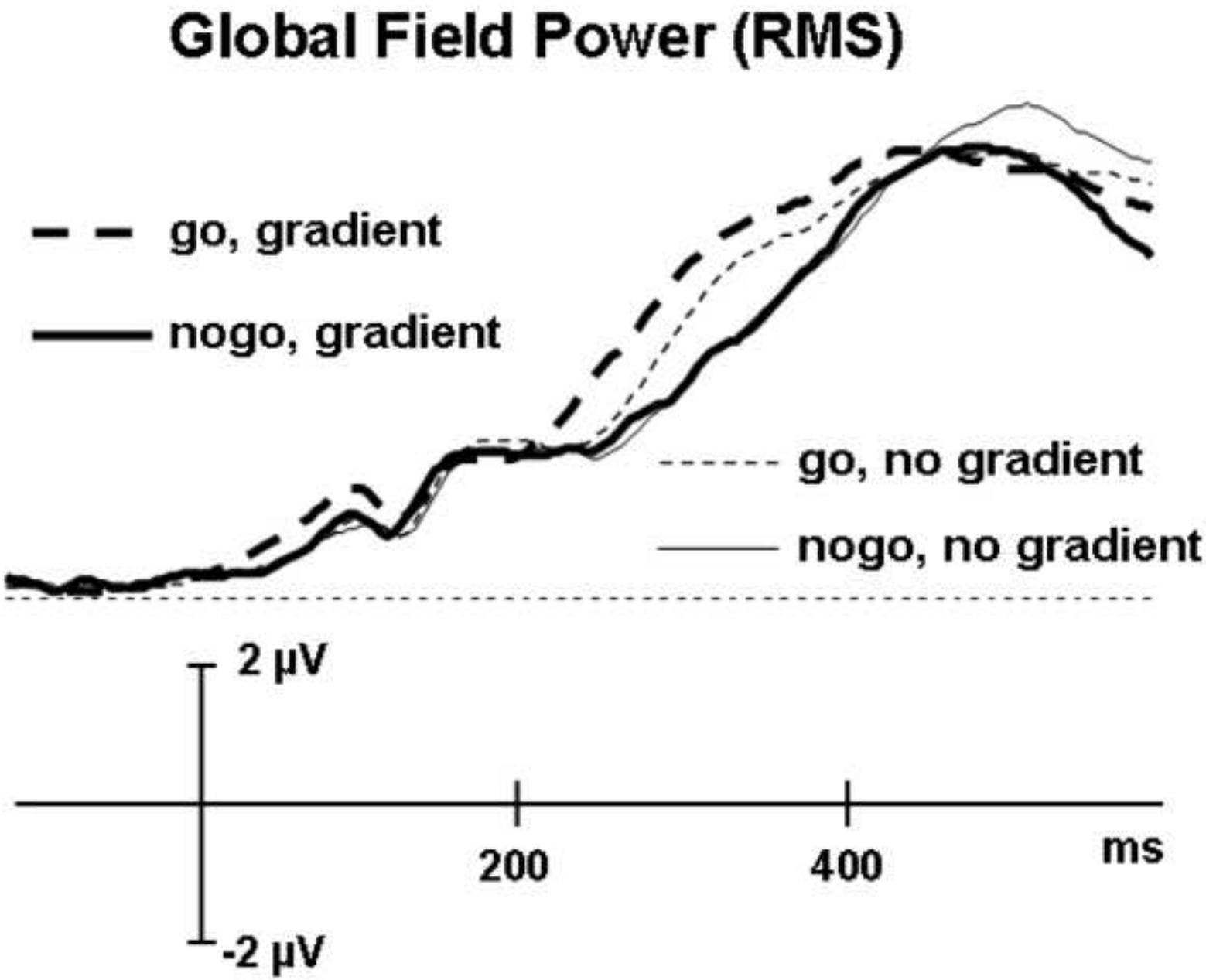

Figure 3

Click here to download high resolution image

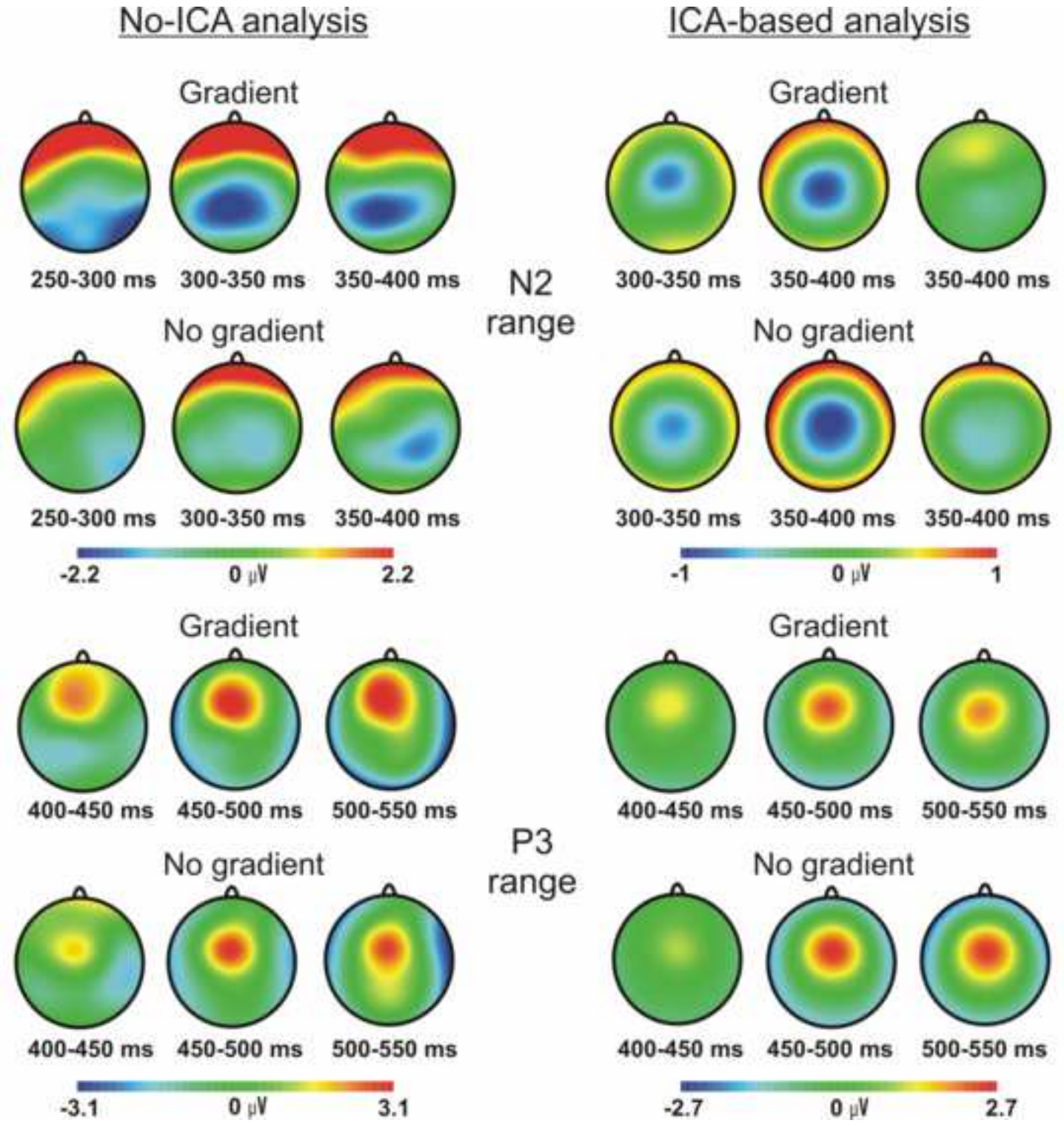

Figure 4

Click here to download high resolution image